JOURNAL OF Applied Polymer SCIENCE

Scrutinizing the Influence of Strain-Induced Fiber Orientation on the Melt Rheological Behavior of Short Aramid Fiber/Thermoplastic Elastomer Composite Using Rubber Process Analyzer

G. S. Shibulal, K. Naskar
Rubber Technology Centre, Indian Institute of Technology, Kharagpur-721302, West Bengal, India
Correspondence to: K. Naskar (E-mail: knaskar@rtc.iitkgp.crnet.in)

ABSTRACT: The effect of fiber loading and its orientational changes on the melt rheological behavior of a short aramid fiber reinforced ethylene-octene copolymer was explored as function of dynamic strain and frequency using a Rubber Process Analyser (RPA). The rheological responses such as the storage modulus and complex viscosity to a cyclic dynamic strain sweep and subsequent linear viscoelastic (LVE) frequency sweep were performed to probe the orientational changes of the short fiber within the sample. An enhanced elastic shear modulus was observed at the low strain regime with a few numbers of repeated strain sweeps and level off thereafter. This can be attributed to the orientational changes of the short fiber from an initial random orientation to a well-ordered concentric fiber string and the string–string packing with repeated oscillatory shear strain. The complex viscosity measured as a function of LVE frequency sweep having the influence of a pre strain history was also found to increases in first few cycles, but very interestingly the complex viscosity measured at all the frequency sweep cycles shows similar values, which are not subjected to any strain history. The optical microscopic images of the samples before and after the RPA analyses clearly support the possibility of fiber orientations and their subsequent packing with repeated strain sweeps. © 2012 Wiley Periodicals, Inc. J. Appl. Polym. Sci. 128: 4151–4163, 2013

KEYWORDS: fibers; composites; rheology; rubber; viscosity; viscoelasticity

Received 28 June 2012; accepted 18 September 2012; published online 18 October 2012
DOI: 10.1002/app.38600

INTRODUCTION

Thermoplastic elastomer (TPE) combines the processing advantages of thermoplastics and the performance advantages of elastomers without the addition of any vulcanizing agent. Ethylene octene copolymer (EOC) is a new class of polyolefin-based elastomeric materials, which have recently gained much attention in numerous application areas. The use of this polymer has been tested very successfully as an impact modifier for both commodity thermoplastics like poly propylene and engineering thermoplastics like PET, Nylon, Poly-oxy methylene (POM), etc.[1–5] However, it seldom finds a position as a promising candidate for load bearing and high temperature engineering applications owing to its poor mechanical, dimensional, and thermal stability. Reinforcing EOC with suitable reinforcing agents that can enhance both strength and thermal stability is one of the ways to circumvent this problem. As far as the short fiber reinforcement of polymers are concerned with an aim of improving both mechanical and thermal stability of weak polymers like EOC, aromatic polyamide, or aramid is one of the potential candidates. These fibers have unique combination of strength, stiffness and thermal stability. However, it shows lesser adhesion with the polymer matrix.[6] Literatures are scanty regarding the reinforcement aspects of EOC with short aramid fiber. Very recently the authors have reported the effect of fiber loading and aspect ratio on the mechanical and morphological characteristics of a RFL coated aramid short fiber reinforced ethylene octene copolymer.[7] The use of a low molecular weight maleic anhydride adducted polybutadiene (MA-*g*-PB) was explored as an interface modifying coupling agent for solving the compatibility problem due to the polarity mismatch between the polar functionalized fiber and the nonpolar EOC matrix as well as to improve the ease of dispersion of aramid fiber with a high aspect ratio into the polymer matrix.[8] It has been recognized that addition of fillers to polymer brings changes in the processing behavior because of the unusual rheological effects.[9,10] The presence of filler increases the melt viscosity leading to increase in the pressure drop across the die but gives rise to less die swell due to decreased melt elasticity. The decrease in the melt elasticity may lead to melt fracture probably at a lower shear rate which would otherwise expect to happen at higher shear rate. Melt fracture is a serious polymer instability that limits the rate of production in many processes such as profile extrusion, film casting, film blowing etc. As a result of this polymer instability,

Table I. Technical Specifications of RFL-Coated Aramid Short Fiber

Parameter/properties	Value
Color	Gold
Specific gravity	1.39
Equillibrium moisture regain (%)	2
Average Fiber length (mm)	3
Diameter (μm)	10–12
Average aspect ratio (*L*/*D* ratio)	275
Young's modulus (GPa)	20–21
Tensile strength (MPa)	3000–3500
Elongation at break (%)	5–7

the final product becomes unattractive and commercially unacceptable. Thus the understanding of the melt rheological properties of the filled polymer system is very much essential to predict and clearly understand the processing behavior and hence to fix the processing parameters to fabricate products. A number of investigations on the melt rheological behavior of short fiber reinforced thermoplastics and elastomers have been reported.[11–13] Generally, incorporation of short fibers onto a polymer matrix increases the melt viscosity and shows complex flow pattern. However, decreases of shear viscosity as a result of the incorporation of short fibers are also reported.[14] It is well known that, unlike in the case of spherical fillers like carbon black, short fiber filled composites produced by conventional injection molding show complex fiber orientation distribution. These fiber orientations can be manipulated by altering the material flow during the mold filling, mold type and processing conditions.[15] The preferential orientations of the fiber cause anisotropy in properties of the composite from molten state to solidification. Thus the mechanical properties of short fiber composite strongly depend on the way in which it is fabricated.

It is very well documented in the literature that when polymer suspensions filled with high aspect ratio fillers (short fibers) are subjected to shear strain in a specified geometrical confinement, the proximity of the fillers lead to a local orientation in the direction of shear strain.[16] Any changes caused by the preferential orientations of the short fiber in the polymer melt can be recognized from the macroscopically observed rheological properties such as viscosity and elasticity. For example, Kim and Song[17] and Kim and Park[18] observed that rheological properties such as complex viscosity (η^*_ω), storage modulus (G'_ω) and loss modulus (G''_ω)for glass fiber reinforced polypropylene decrease with repeated frequency sweep due to the orientations of the glass fiber in an oscillatory shearing flow. Several methods such as stereological measurements, effects of cluster formation etc. have been reported earlier to characterize the fiber orientation within the sample.[19,20] Very recently Fu et al. employed optical microscopy (OM) and scanning electron microscopy (SEM) as direct and simple methods for assessing the shear-induced fiber orientations.[21] In this investigation, an attempt has been made to understand the effect of fiber orientations through rheological response of short aramid fiber filled ethylene octene copolymer using a Rubber Process Analyzer as well as optical microscopic analyses. The first part of the discussion deals with the effects of fiber loading on the rheological properties as a function of dynamic strain amplitude and its correlation with the uniaxial stress–strain behavior of the composite moldings in the unsheared condition. The second part of the article elaborates and explains the rheological behavior of the composite due to the shear induced fiber orientation. Till date no studies has been reported regarding the orientation effects on the melt rheological behavior of any short fiber-filled thermoplastic elastomer in general and ethylene - octene copolymer in particular using a RPA.

EXPERIMENTAL

Materials

Ethylene octene copolymer (trade name EXACT® 5061 (specific gravity of 0.868 g/cc at 23°C; comonomer (octene) content of 13%; melting temperature (T_m) of 52.8°C, melt flow index (MFI) of 0.5 @190°C/2.16Kg was procured from Exxon Mobil Chemical Company, USA. Aramid short fiber (trade name Technora®) with a chemical name copoly-(paraphenylene/3, 4′-oxydiphenylene terephthalamide) was obtained from Teijin Aramid BV, The Netherlands. The detail specifications of the fiber are given in Table I.

Preparation of Composites

The formulation used for the preparation of composites is shown in Table II. All the composites were prepared by melt mixing of the components in a Haake Rheomix 600 OS internal mixer having a chamber volume of 85 cm^3 at a temperature of 80°C with a rotor speed of 80 rpm for 10 min. The short fiber loading was varied from 1 to 10 phr. To achieve better dispersion, half portion of the polymer was first melted for 1 min and to this half portion of fiber was added and the mixing was continued for another 1 min. The sequence is again repeated for 2–3 min with the remaining portion of polymer and the mixing was continued up to10 min after adding the remaining portion of the fiber at 3rd min at a constant rotor speed of 80 rpm. Once the mixing is over, the composite was discharged and passed through a two roll mill once to get a flat sheet. The sheet was then pressed in a compression molding press (Moore Press, Birmingham, UK) at 100°C for 3 min at a pressure of 7 MPa and then cooled down to room temperature under the same pressure by circulating cold water to get randomly oriented fiber composites (composites in unsheared condition).

Characterization of the Composites

Mechanical Properties. The dumb-bell shaped specimens of the composites in parallel and perpendicular directions with respect to the mill direction were die cut from the compression molded sheet and the testing was done after 24 h of maturation at room temperature. Tensile properties were measured according to ASTM D412-98A using a universal testing machine Hounsfield H10KS (UK) at a constant cross-head speed of 500

Table II. Formulations of the Mixes in phr (Parts Per Hundred Rubbers)

Polymer (phr)	100	100	100	100	100
Short fiber (phr)	0	1	3	5	10

mm/min. All the reported values were the averages of three measurements.

Dynamic Rheological Measurement Using Rubber Process Analyzer. The rubber process analyzer (RPA 2000, Alpha Technologies, USA) was employed to study the dynamic rheological properties of the composites. It uses a rotorless, biconical die design that contains two cone-shaped dies. During the test, the lower die sinusoidally oscillates the sample as per the preprogrammed strains and frequencies at controlled temperature while the upper die mounted to a reaction torque transducer measures the complex torque (S^*) and the phase angle transmitted through the sample from the lower die. From the complex torque and the phase angle, a special Fourier transform software program determines the pure elastic torque (S') and the pure viscous torque (S''). From these, the elastic shear modulus (G') and the viscous shear modulus (G'') can be calculated with the applied strain as follows:

$$G\prime = KS'/\text{strain} \quad (1)$$

$$G'' = KS''/\text{strain} \quad (2)$$

where K is a constant related to the geometry of the dies and the sample cavity. The frequency and strain of oscillation can be varied during the test between 0.1–33 Hz and 0.7–1256%, respectively. The temperature can be also programmed to change as fast as 1°C, upward or downward between 40 and 230°C. For this investigation, a dynamic strain sweep was conducted first to determine the LVE region by varying the possible strain ranges of RPA from 0.7 to 1256% at a constant frequency of 0.3 Hz at 80°C. Dynamic frequency sweeps were then carried out from 0.1 to 33 Hz at a constant strain within the LVE region of the material. We have kept a constant strain of 1% for the frequency sweep study because all the fiber-loaded composite shows an LVE regime within this strain range.

Fiber Orientation Studies. To understand the effect of strain induced fiber orientation on the melt rheological behavior of the composite we have performed a repeated amplitude sweep, repeated frequency sweeps and repeated frequency sweeps immediately after strain sweep (amplitude dependant frequency sweep) on a specific fiber loaded composite as per the following program.

Program No. 1: Cyclic strain sweep. The strain is varied from 0.7% to a desired extent of strain (say 100, 500, and 1256%) by keeping a constant frequency of 0.3 Hz at the test temperature. After every sweep the sample is cool down to 40°C and kept at this temperature about 3 min and again heated to the test temperature by keeping the sample within the test cavity of RPA for the next strain sweep cycle.

Program No. 2: Cyclic frequency sweep. The frequency is varied from 0.1 to 33 Hz at the test temperature and a constant LVE strain of 1%. Here also after every frequency sweep cycle, the temperature is reduced to 40°C, keeping the sample within the confines of the cavity of RPA for about 3 min and again heated to the test temperature for the next frequency sweep cycle.

Program No. 3: Cyclic frequency–strain sweep. An LVE frequency sweep was first conducted at the test temperature by varying the frequency from 0.1 to 33 Hz at a constant strain of 1%. Then the frequency is reduced from 33 to 0.1 Hz with in 30 s and immediately performed a strain sweep of desired strain range at the same temperature. After the measurement of a frequency sweep and strain sweep together in one cycle, the sample is cool down to 40°C and kept at this temperature for about 3 min and again heated to the test temperature by keeping the sample within the cavity of RPA for the next cycle. Each measurement was performed on a fresh compression molded sample and repeated measurements had been taken to ensure the reproducibility of the experimental results.

Morphological Analyses Using Optical Microscopy. To examine the orientational changes in the short fiber filled EOC with repeated strain sweep measurements, after every strain sweep, the test sample was taken from the rheometer die without any damage and cut a small portion few mm away from the center of the sample and analyzed by optical microscope (Leica DMLM, Germany) with a magnification of X5. An optical microscopy of the sample was also taken before any rheological measurement at the same magnification for one to one comparison with the sample after the rheological experiment.

RESULTS AND DISCUSSION

Effects of Fiber Loading and Dynamic Shear Strain on Shear Storage Modulus

Figure 1(a) shows the semi-log plot of the variation of shear storage modulus (G') of the native matrix and its short fiber-loaded composite as a function of oscillatory shear strain varying from 0.7 to 1256%. The native matrix shows an LVE region up to a strain level of 39%, where the storage modulus was independent of strain followed by a nonlinear viscoelastic (NLVE) regime where the G' continuously decreases as a function of strain amplitude. An augmentation in the modulus was noticed at the LVE regime of the native matrix with increase in the short fiber concentration; which indicates the reinforcement effect of the aramid short fiber.[22] Earlier many researchers have proved that the reinforcement of polymer with any kind of filler is a combined contribution of the filler–filler and filler–matrix interaction and these interactions generally will strongly affect the rheological properties as well.[23–26] In the present system, as the two components show polarity mismatch, the reinforcement may arise mainly from the high level of fiber network formation owing to its high aspect ratio and also from the mechanical interlocking between the rough aramid fiber surface (due to resorcinol formaldehyde latex (RFL) coating) and the polymer.[7] With increase in the concentration of the short fiber, it creates a fiber network inside the matrix owing to its inherent polar nature and the ability to form inter H-bonding. Here the polarity and the interaction between the aramid fibers are perhaps more due to RFL coating since it creates more polar functionalities on the fiber surface.[27] It has also been noted that the LVE region of the neat EOC is getting reduced with the addition of short fibers and is continuously reduces as the short fiber content increases. For example, the LVE region of the neat EOC reduces from 39 to 3% at a fiber loading of 10 phr. This

Applied Polymer SCIENCE

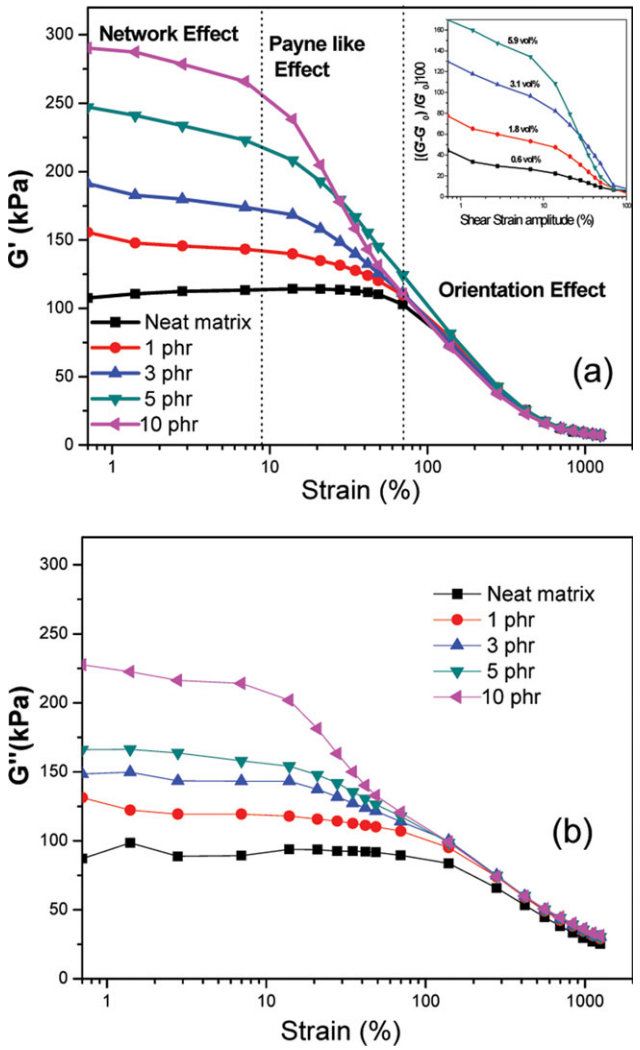

Figure 1. Variation of shear moduli with short fiber loading as a function of shear strain amplitude from 0.7 to 1256% at a constant frequency of 0.3 Hz at 80°C. (a) G' versus strain amplitude and (b) G'' versus strain amplitude. [Color figure can be viewed in the online issue, which is available at wileyonlinelibrary.com.]

immediate decrease in the LVE regions of the composite has a striking analogy with the "Payne effect," which is generally observed in highly carbon black filled or silica filled elastomers at very high volume percentage (>20%). Payne effect is basically the reduction of dynamic storage modulus due to the breakdown of the filler network with increasing dynamic strain.[28,29] In this investigation, we observed a pronounced "Payne like effect" at a short fiber concentration of 3 vol %, but actually it starts even at a fiber loading as low as 1 vol % (more precisely at 0.6 vol %), which is much lesser than the volume fraction of spherical fillers like carbon black or silica to show the same effect. This can be attributed to the network formation of the aramid fiber even at low concentration owing to its high aspect ratio and polarity followed by the network disruption with growing strain amplitude. The inset of Figure 1(a) shows the percentage improvements in the storage modulus with short fiber loading as a function of strain. It is clear that the moduli of the composite were always higher than that of the native matrix up to a strain level of 10%. This is because the network formed by the aramid fiber is strong enough to undergo any kind of disruption in the low amplitude region. In other words, the rate of disruption and the reconstruction of the fiber network exist in a reversible manner at low deformation. This elastic behavior of the rigid fiber network in the composite enhances the storage modulus.[31] However, the composite moduli were gradually dropped down almost to the modulus of native matrix at a strain of 100% due to disruption of the fiber network. It is worth noting from the Figure 1(a) that a sharp declination in the storage modulus (strain softening) was observed at a strain greater than 100%, beyond which the neat matrix and the composite show almost same modulus value irrespective of the short fiber loading. This sharp strain softening can be attributed to the combined effect of the disentanglement of the polymer chains and the orientation of the short fibers at extremely high strain.[22,30] The behavior of storage modulus with short fiber loading observed at the low strain and the growing strain amplitude is very well corroborated with the uniaxial stress–strain behavior of the composite as a function of fiber loading. Figure 2 shows the tensile modulus versus tensile strain plot of the native matrix and its composite as a function of fiber loading. It demonstrates the modulus at different strain percentage. Here also we noted an augmentation in the tensile modulus with fiber loading and that got declined with growing strain as observed in the case of the variation of shear storage modulus as a function of growing strain amplitude. These similar trends in tensile modulus with short fiber loading as a function of strain very well substantiate the existence of fiber network in the low strain regime, its disruption in the medium strain and its orientation in the high strain regimes. It is very interesting to note from Figure 3, which represents a general engineering stress versus strain plot (the inset shows its linear scale) as a function of short fiber loading, a strain hardening (increase in the stress owing to the alignment of polymer chain and the short fiber in the direction of the applied strain) at a strain

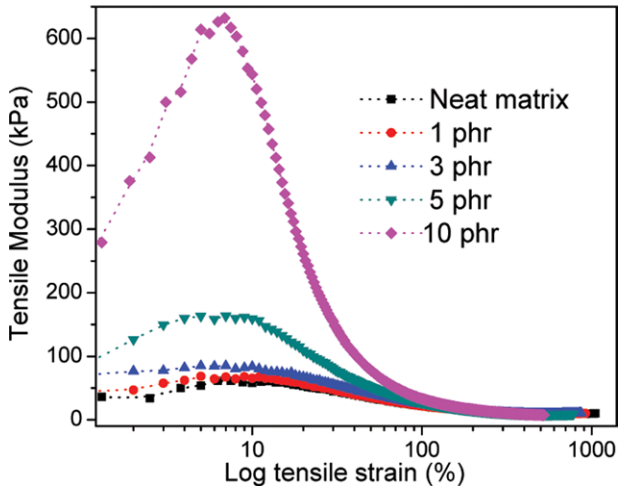

Figure 2. Tensile modulus versus tensile strain plot as a function of short fiber loading. [Color figure can be viewed in the online issue, which is available at wileyonlinelibrary.com.]

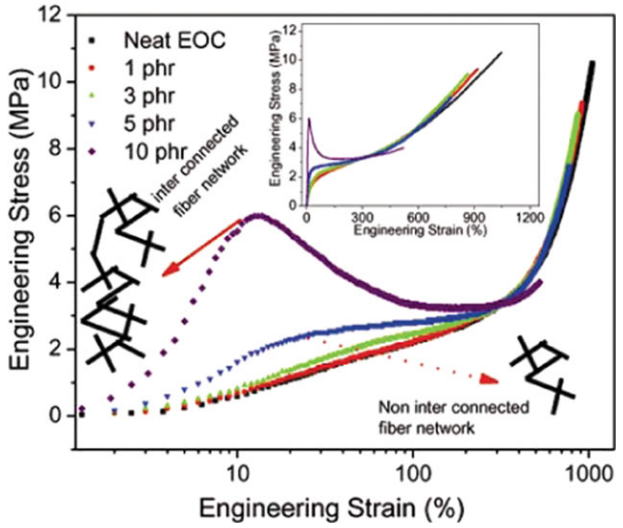

Figure 3. Engineering stress versus engineering strain plot of neat EOC and its composite as a function of short fiber loading (inset shows the same in linear scale). [Color figure can be viewed in the online issue, which is available at wileyonlinelibrary.com.]

greater than 300%. This was true only up to a short fiber loading of 5 phr. This is because the network formed by the short fibers up to a loading level of 5 phr is not sufficient to form any percolation cluster (interconnected continuous fiber network) due to low average number of fibers per unit area. Hence, most of the networks developed up to a fiber loading of 5 phr may be a noninterconnected one and the interaction across the fiber–fiber crossing may be weak as it is connected through a physical attraction. Whatever the noninterconnected network being formed up to 5 phr fiber loading is broken up very easily and starts to align in the direction of applied strain results in an homogenous deformation like neat EOC and shows a strain hardening effect beyond a strain of 300%.[31] However, as the short fiber loading increases to 10 phr, the average number of fibers per unit area increases which leads to the formation of a well-interconnected fiber network and hence achieved the percolation threshold. This interconnected fiber network is very strong enough to bear more load whose fracture requires much higher energy, which is responsible for the sharp jump in the tensile modulus as well as shear modulus at this fiber concentration.

Strain Dependence of Viscous Modulus (G″) as a Function of Short Fiber Loading

Figure 1(b) represents the response of the viscous modulus as a function of strain amplitude with short fiber loading. The loss moduli were found to increase at the low strain region with short fiber loading essentially similar to the behavior observed for the storage modulus with fiber loading. However, the magnitude of loss moduli of both the native and composites were always lower than its corresponding G' values at the low strain regimes. However, an upturn in their behavior was observed at a strain greater than its cross-over strain. Figure 4 represents the dynamic intersection (cross-over) of storage and loss modulus of both native matrix and its composites (for clarity, only 1 and 10 phr fiber-filled composites are shown here) as a function of strain amplitude. The cross-over strain was found to decrease and moves towards the low strain region with increase in fiber loading. For example, with the addition of 1 phr of short fiber, the loss modulus overtakes the storage modulus at a strain of 71.8%, whereas the two moduli intersect at a strain of 44% for 10 phr fiber-loaded composite. This means that the elastic region of the composite gets reduced as a matter of both fiber loading and with growing strain. Once the strain amplitude is high enough so that the fiber network is destroyed to such an extent that it cannot be reconstructed in the time scale of dynamic strain (0.33 Hz).[32] This broken fiber networks behaves like a noninteracting rigid rods suspended in a Newtonian liquid, since all the polymer chains become uncoiled at very high strain responsible for the upper Newtonian region. This fiber-network disruption and the polymer chain disentanglement (chain orientation) results higher free volume, which enhances the viscous component as evidenced from the increased G'' at this strain regime.[33] This high viscous modulus beyond the cross-over strain increases the damping efficiency (tan δ) of the composite, which is the ratio of loss to storage modulus (tan $\delta = G''/G'$). Tan δ of the composites were found to decrease well below the cross-over strain (≈10% strain) with short fiber loadings, indicating the existence of a strong short fiber network and its elastic contribution (increased storage modulus) to the composite. However, tan δ increases with fiber loading well above the cross over strain (1000%) due to the dominating effect of the viscous component. The behavior of tan delta at 2% and at 1000% strain as a function of fiber loading are showed in Figure 5.

Rheological Evidences for the Strain-Induced Fiber Orientations

From our analyses on the behavior of shear storage modulus (G') to amplitude sweep with various fiber loading, it has been apparently observed that at a strain beyond 100%, the G' of all the composites behave similar to that of the native matrix due

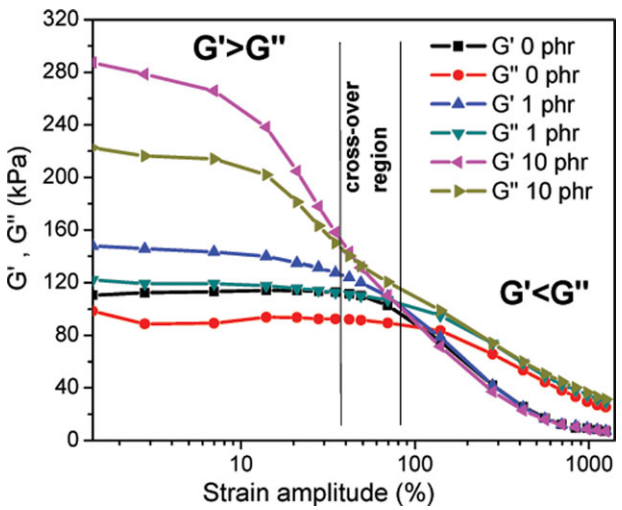

Figure 4. The dynamic intersection between G' and G'' with shear strain amplitude as a function of short fiber loading. [Color figure can be viewed in the online issue, which is available at wileyonlinelibrary.com.]

Applied Polymer SCIENCE

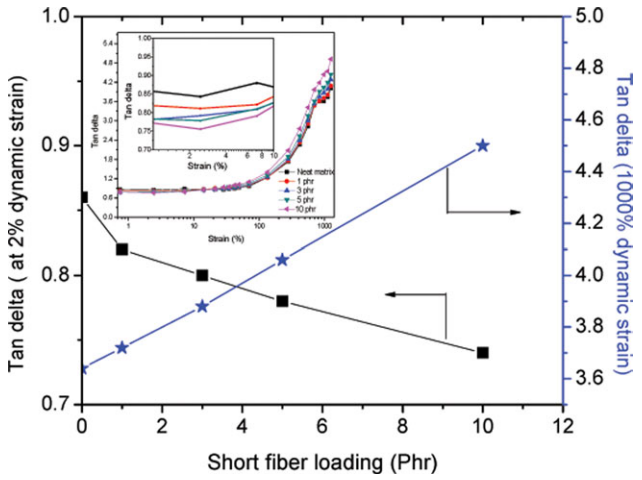

Figure 5. Variation of tan delta as a function of short fiber loading at 2% strain and at 1000% strain. (Inset shows tan δ as a function of strain sweep). [Color figure can be viewed in the online issue, which is available at wileyonlinelibrary.com.]

to the orientation of the fiber beyond this strain level. To understand the effect of this fiber orientation on the low strain shear modulus and also up to what extent of strain is really responsible for the maximum fiber orientation, the experiments were done as per the preprogrammed testing protocols as discussed in the experimental section. The neat polymer and a 5 phr fiber-loaded composite have been taken for the detailed analyses and a one to one comparison was made to understand the effect of strain induced fiber orientations. The reasons for the selection of 5 phr fiber-loaded composite are that it offers a balanced mechanical properties and a good quality of fiber dispersion without any dispersing agent.[8] Moreover, at this fiber loading the formations of a well-interconnected fiber network is not possible, which helps to understand the orientation effect very nicely.

(a) Effect of repeated strain sweeps on the shear moduli (G' and G'').

Figure 6 represents the G' and G'' of the native matrix with repeated strain sweeps from 0.7% to 1250%. It can be seen that the linear to nonlinear behavior of both the G' and G'' in all the four strain sweep cycle were almost close to each other. However, the magnitude of G'' for all the four cycles were lower than their corresponding G' values up to a dynamic cross-over strain (γ_c) of 72%. This reversible behavior of the G' in all the four cycles of strain sweeps may be due to the good elasticity and quick elastic recovery of EOC even after a serious of cyclic deformation, which is confirmed by more or less similar cross-over strains for all the four strain sweep cycles. An upturn in the loss to storage modulus was noticed beyond the cross-over strain, which is due to the higher viscous component owing to the disentanglement of the polymer chain leading to a less elastic modulus. Figure 7(a) represents the variation of G' of a 5 phr fiber-filled EOC with repeated strain sweep from a strain of 0.7% to 1250% in four cycles. An augmentation in the shear storage modulus was noted in the low strain region after each sweeps just like the increase in the modulus with fiber loading. However, the G' approaches a constant value beyond the third cycle. This can be explained as follows: during the first strain sweep, the G' at the low strain regime is mainly controlled by the network created by the short fiber in the matrix. As the strain grows the fiber network gets broken down and starts to orient along with the coiled polymer chain. When the shear strain range is form 500 to 1250%, the coiled polymer chains undergo a full disentanglement, which helps to orient more amounts of short fibers that got oriented when the oscillatory strain was in the range of 0.7–500%. It is intuitively expecting that due to the repeated oscillatory shear deformation, whatever the short fibers already aligned come close and connected to each other endwise to form a continuous concentric fiber string inside the sample preferably in the strain range of 500–1250%. Such a well-connected continuous fiber string structure gives high strength to the composite. Any further strain sweep performed on the sample at this condition may help to stack the continuous fiber strings already formed from the discontinuous fibers. This tightly packed fiber string structure may further strengthen the composite, which offers more shear resistance in the direction of the oscillatory shear strain, which is quite evident from the continuous increase in the shear storage modulus from the first strain sweep cycle to the third cycle. Once the fiber string packing attains a steady state, any further shear deformation will never cause significant changes in the shear storage modulus. This may be one of the reasons why we observed almost similar shear storage modulus in the 3rd and 4th cyclic deformation. A schematic representation demonstrating the state of the oriented fiber structure within the sample before performing each amplitude sweep from 0.7 to 1250% is also shown in Figure 7(a). Figure 7(b) represents the variation of G' with repeated oscillatory shear strain from 0.7 to 100%. It is clear from the figure that the G' measured during the first strain sweep was always higher than that measured during the subsequent sweeps. This is because the periodical strain ranges from 0.7 to 100% imposed on the composite is not good enough to

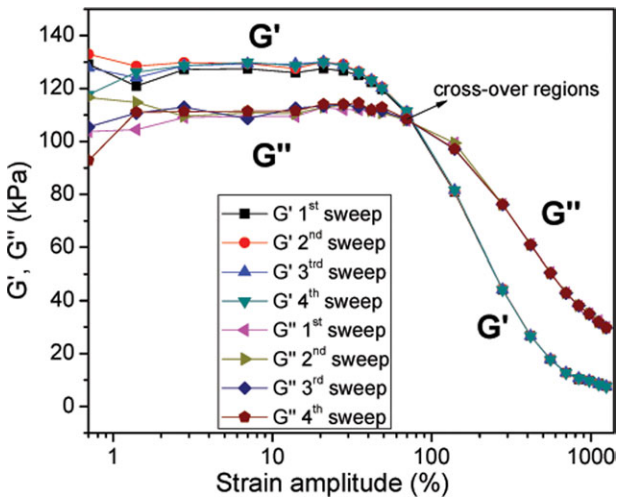

Figure 6. Variation of G' and G'' of the neat EOC with repeated strain sweeps from 0.7 to 1256%, 0.3 Hz at 80°C. [Color figure can be viewed in the online issue, which is available at wileyonlinelibrary.com.]

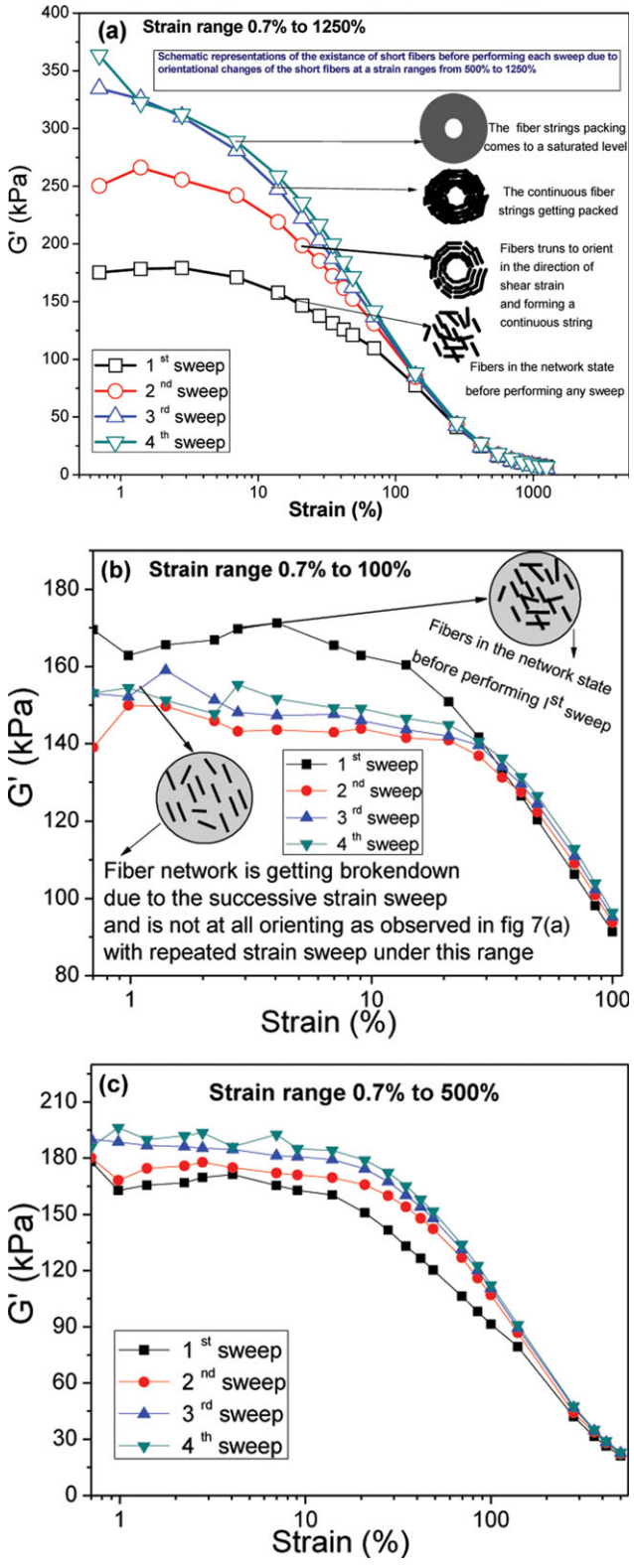

Figure 7. Variation of G' of a 5 phr short fiber-filled composite with repeated strain sweeps of various strain ranges at 80°C and 0.3 Hz (a) sweep with strain range 0.7–1250% (b) 0.7–100%, and (c) 0.7–500%. [Color figure can be viewed in the online issue, which is available at wileyonlinelibrary.com.]

destruct the network structure created by the interdigitated flexible aramid short fibers into a fully oriented state. Moreover, whatever the small quantity of fibers getting oriented with repeated strain sweeps under this strain range is not effective to develop a continuous fiber string structure within the composite. Thus the shear storage modulus due to the network effect (modulus measured during the first strain sweep) is always higher than that measured during the subsequent strain sweep. Figure 7(c) represents the variation of G' with repeated oscillatory shear strain from 0.7 to 500%. It is worth noting that the G' measured during all the four strain sweeps follows the order $G'_4 > G'_3 > G'_2 > G'_1$ as observed in the case of the repeated strain sweep ranges from 0.7 to 1250%. This can be attributed that the orientation of the discontinuous fiber and the subsequent continuous fiber formation under this strain range is much more pronounced than it was in the range of 0.7–100%. However, the magnitude in the modulus growth with repeated strain sweep was less unlike in the case of the repeated strain sweep ranges from 0.7 to 1250%. This may be due to the fact that the repeated oscillatory strain under this range (0.7–500%) imposed on the sample is not sufficient to develop a tightly packed concentric fiber string as observed when the repeated oscillatory strain was in the range of 0.7–1250. The low strain moduli measured in the first strain sweep cycle (G'_1) and that measured in the fourth strain sweep cycle (G'_4) at different extents of strain is given in Table III. For uniformity, the moduli measured at a strain of 2% have been taken for the comparison. Here the modulus measured in the first strain sweep cycle can be thought of a network shear modulus, since fiber network formation is the contributing factor for the initial oscillatory shear resistance. On the other hand, the moduli measured in the fourth cycle can be thought of orientation shear modulus because in such case the resistance to shear strain is contributed by oriented fiber structure. It is clear from the table that the application of a repeated oscillatory shear strains in the range of 0.7–500% on the composite increases its low strain storage modulus by about 14% and is further increased to 87% when the oscillatory shear strain in the range of 0.7 to 1250%. However, the application of a strain ranges from 0.7 to 100%, reduces the initial storage modulus of the composite by about 12% due to the fiber network break-down and the inability to form a strong fiber string.

The variation of loss moduli (G'') of the composite with repeated strain sweeps in the range of 0.7 to 1250% were almost same as in the case of the variation of G' with repeated amplitude sweep. However, the magnitude of G'' were always lower than their corresponding G' value obtained in the respective strain sweep cycle up to their dynamic cross-over strains (γ_c). Beyond the cross-over strain an upturn in the magnitude of loss to storage modulus has been observed. Figure 8 represents the dynamic intersection of G' and G'' for the first strain sweep and the 4th strain sweep cycle. For clarity, those obtained for the 2nd and 3rd strain sweep cycles have been omitted however its cross-over strains are indicated in the inset table of the same figure. It is very interesting to note that, the cross-over strain is gradually decreasing as the number of cyclic deformation increases. As per the viscoelastic theory, G' represents the solid

Table III. Changes in the Low Strain Storage Modulus Due to Repeated Strain Sweeps at Different Extents of Strains

	Strain sweep ranges		
Storage modulus at 2% strain (kPa)	0.7–100%	0.7–500%	0.7–1256%
G'_1 (kPa)	169.5 ± 4.6	169.5 ± 4.6	169.5 ± 4.6
G'_4 (kPa)	149.5 ± 2.0	193.5 ± 1.8	318.7 ± 2.3
$\Delta G' = (G'_4 - G'_1)/G'_1$ (%)	−11.9	14.0	87.4

G'_1 represents the shear storage modulus for the first strain sweep cycle and G'_4 that of the fourth strain sweep cycle.

behavior of the material, G'' indicates the viscous nature (liquid behavior) and their ratio (G''/G'), which is known as the "damping factor" denotes the relative stiffness of the material. If we analyze the behavior of these rheological parameters with repeated strain sweeps on the basis of the viscoelastic theory, we can say that the solid behavior (elastic modulus) of the composite is getting increased and the extent of solidity is getting reduced as the no of cyclic deformation increases. This is evident from the successive reduction in the cross-over strain with repeated cyclic deformation. As discussed earlier, a strong fiber string is developed within the composite under this strain range which is getting strengthened with further strain sweeps due to the stacking interaction between the oriented fiber strings. This well oriented and the tightly packed fiber string in the composite offers a very high shear resistance in the low deformation region which naturally enhances the G' value. With the repeated cyclic deformation, the polymer bounded over the well-oriented fiber string may gets weakens which reduces its ability to hold the fibers firmly. As a result, the viscous component such as the loss modulus (G'') increases, which ultimately reduces the strain at which the dynamic intersection between G' and G'' with the increased number of cyclic deformation. Figure 9 represents the loss factor (tan δ) of the composite with repeated strain sweep cycle. Up to a strain level of 10%, the behavior of tan δ measured from Ist strain sweep cycle to IVth cycle follows the order I > II > III > IV. However beyond a strain of 10%, an upturn in the magnitude of tan δ was observed and it follows the order I < II < III < IV. For example, the magnitude of tan δ observed at a strain of 2% and at a strain of 1000% for the first strain sweep cycle to the fourth cycle is shown in the inset table of Figure 9. The gradual reduction in the tan delta value from the first cyclic deformation to the fourth cyclic deformation in the low strain region (up to 10%) again substantiate the fact that the increased stiffness of the composite in the low deformation region due to the formation of a strong continuous fiber string. At very high strain both the short fiber and the polymer chain will be fully in the unfolded oriented state. This simultaneous polymer chain orientation and the fiber orientation results in the formation of some large unoccupied regions in the composite.[33] The formation of such large unoccupied regions in the composite increases the viscous component and hence the tan delta also increases.

(b) Effect of the sequential application of two different strain ranges on the shear storage modulus.

From the repeated strain sweep study with three different strain ranges it has been confirmed that the short fibers turn to a

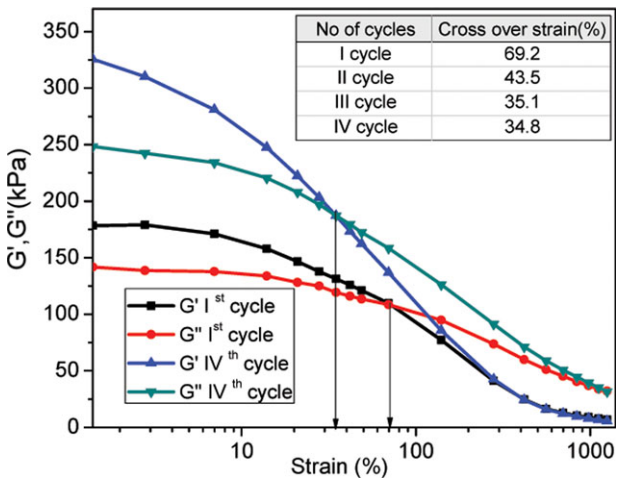

Figure 8. Dynamic intersections between G' and G'' during the 1st strain sweep and 4th sweep of a 5 phr short fiber composite in the strain range of 0.7–1256 %, at 80°C. (Inset shows the crossover strains at different cycles). [Color figure can be viewed in the online issue, which is available at wileyonlinelibrary.com.]

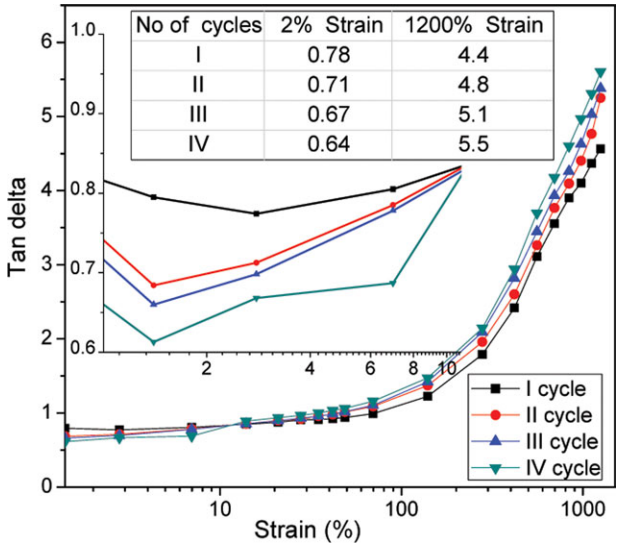

Figure 9. Variation of the damping factor (tan delta) of a 5 phr short fiber loaded composite with repeated strain sweep from 0.7 to 1256% at 80°C. [Color figure can be viewed in the online issue, which is available at wileyonlinelibrary.com.]

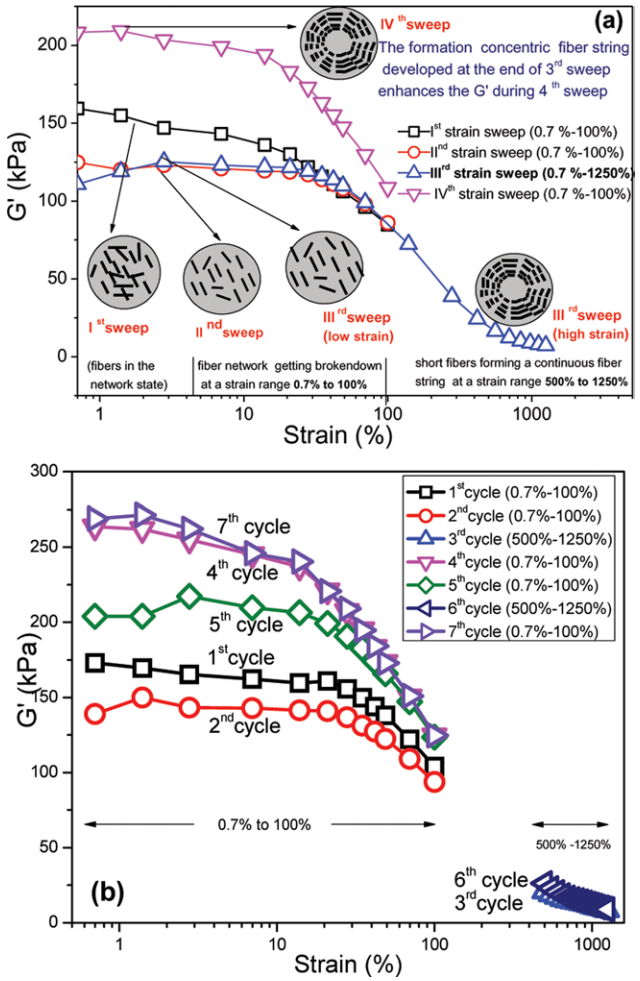

Figure 10. Variation of G' of a 5 phr short fiber composite by the simultaneous application of a combination of repeated strain sweeps (a) combination of strains 0.7–100% and 0.7–1250% and (b) combination of strains 0.7–100% and 500–1250%.[Color figure can be viewed in the online issue, which is available at wileyonlinelibrary.com.]

strong continuous fiber string in the circumferential direction during the strain ranges from 500 to 1250%. To further substantiate this observation, we applied a combination of two different oscillatory strain ranges such as 0.7–100% and 0.7–1250% in different sequences on the sample which is under investigation. First, we applied two successive strain sweep cycles in the range 0.7–100% followed by a third cycle in the range from 0.7 to 1250%. The fourth cycle was again in the range of 0.7–100%. The shear storage modulus measured during each strain sweeps have been shown in Figure 10(a). It is very clear from the figure that the changes in the shear storage modulus at the low strain regime during the first three strain sweep cycles were similar to the behavior we have already explained for Figure 7(b). However, a sudden growth in the storage modulus was noted in the low strain region during the 4th strain sweep. This modulus growth during the 4th strain sweep cycle was not observed when it is measured after applying a strain sweep (3rd strain sweep) ranges from 0.7 to 100%. Instead it was always below the modulus recorded during the first strain sweep cycle [see Figure 7(b)]. These results once again substantiate the formation of a strong continuous fiber string in the circumferential direction during the oscillatory strain ranges from 500 to 1250%. A schematic representation of orientational changes in the short fiber with the application of each strain sweeps are also depicted as an inset in Figure 10(a). Figure 10(b) also explains the variation of G' with sequential application of a combination of strain sweeps ranges from 0.7 to 100% and 500 to 1250% in seven cycles. The responses of G' to the first four cycles were exactly similar to that observed in Figure 10(a). It is important to note from the figure that G' measured during the 5th strain sweep comes in between the 4th and the 1st strain sweep cycles. This can be attributed that the fiber string formed by the application of 3rd strain sweep is getting collapsed due to the successive application of the 4th strain sweep under the strain range of 0.7–100%. Hence, again if we apply an immediate strain sweep under the same range incapable of fiber string formation, naturally the storage modulus (G') will decrease that is what we have observed here. It is interesting to note that when we again applied an oscillatory strain sweep in the range of 500–1250% (capable of forming a continuous fiber string within the composite) after the 5th sweep, the storage modulus at the low strain region again goes up and merge with the 4th cycle. This may be due to the reconstruction of the collapsed fiber string due to the effect of the 6th strain sweep cycle under the strain rage of 500–1250%.

(c) Effect of strain history on the complex viscosity of the composite with repeated frequency sweeps.

To understand the effect of strain induced fiber orientation on the complex viscosity of the composite as a function of frequency, we conducted a frequency sweep immediately after a strain sweep as per the testing protocol No. 3 detailed in the experimental section. All the frequency sweep experiments were repeated in four cycles by varying the frequency from 0.1 Hz to 33 Hz at a constant LVE strain of 1%. For comparison a frequency sweep experiment was also performed on the composite without the effect of any previous strain history as per program No. 2 and the complex viscosities measured are displayed in Figure 11(a). Figure 11(b,c) also represents the variation of complex viscosity as a function of angular frequency. Here except the complex viscosity measured in the first frequency sweep cycle, all others have various extents of prestrain histories. For example, the complex viscosities shown in Figure 11(b) are measured immediately after a strain sweep from 0.7 to 100%. Similarly complex viscosities shown in Figure 11(c) are also measured immediately after a strain sweep from 500 to 1250%. It is clear from Figure 11(a) that the complex viscosities measured at all the four frequency sweep cycles were almost similar and shows a pseudoplastic behavior with increasing the frequency. From Figure 11(b) it is clear that the complex viscosity measured during the first frequency sweep cycle was always higher than those measured during the subsequent frequency sweep cycles throughout the whole frequency range from 0.1 to 33 Hz. On the other hand, it is very clear from Figure 11(c) that, the complex viscosity measured during the second frequency sweep cycle was higher than that measured during the first frequency sweep cycle and it was still higher for the 3rd

Applied Polymer SCIENCE

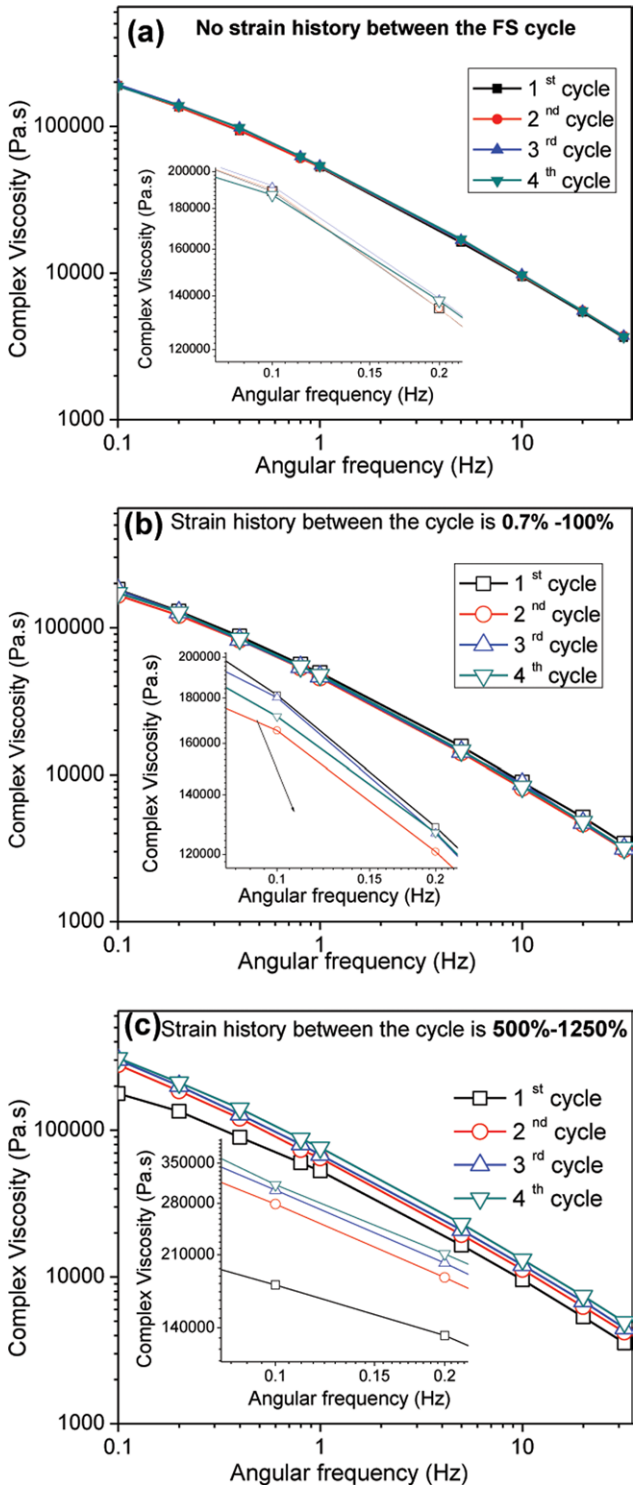

Figure 11. Variation of complex viscosity of the composite with repeated frequency sweep from 0.1 to 33 Hz at a constant strain of 1% at 80°C involved with different extent of strain histories. (a) No strain history (b) 0.7–100% (c) 500–1256%.[Color figure can be viewed in the online issue, which is available at wileyonlinelibrary.com.]

frequency sweep cycle throughout the whole frequency sweep range. However, it shows no further significant changes after the 3rd frequency sweep cycle. We have already noted that an oscillatory shear strain from 0.7 to 100% does not make any significant fiber orientations of the detached fibers from its network connectivity. Moreover, under this oscillatory shear strain no effective fiber string formation is taking place as mentioned in the above section. As a result, the complex viscosities measured with repeated frequency sweeps having pre-strain histories of these strain ranges shows a lower value at the entire frequency sweep. However, a considerable fiber orientation and an endwise connectivity between the oriented fibers are possible as the dynamic oscillatory strain extended from 100 to 500%. Once the strain reaches to 1250 from 500%, the short fibers within the composite forms a concentric fiber string in the circumferential direction. This may lead to a kind of *in-situ* cord reinforcement in the circumferential direction of the composite, which is evident from the increased storage modulus with repeated strain sweep under this strain range. Thus if we measure the complex viscosity immediately after the application of a strain sweep capable of the above said concentric fiber string formation will be always higher than those measured without any such strain history.

Effect of Temperature on Fiber Orientation

To understand the effect of temperature on the fiber orientation and the subsequent effect on the shear storage modulus and the complex viscosity, a cyclic strain sweep(as per program No. 1) and a cyclic amplitude dependent frequency sweep (as per the program No. 3) were performed at two other temperatures such as at 60 and at 100°C. Figures 8, 12(a) and 12(b) represent the variation of G' and G'' with repeated amplitude sweep from 0.7 to 1250% at 60, 80, and 100°C, respectively. The magnitudes of both the G' and G'' were found to decrease with increase in temperature. However G' was always higher than their corresponding G'' up to their cross-over points at 60 and 80°C. Whereas G'' was found always higher throughout the whole strain range at a temperature of 100°C, after C. These observations are expected because at lower temperature the stiffness of the composite will be more and hence it shows higher G' value. It is important to note from Figure 12(a) that the G' measured during the first strain sweep was always higher than that measured during the subsequent strain sweeps. This is similar to the behavior we have already observed in the case of the variation of G' with repeated strain sweeps from 0.7 to 100% at 80°C. This can be attributed to the fact that the composite viscosity is much higher at 60°C, which makes a strong resistance to orient the short fibers in the direction of the applied oscillatory strain even if it ranges from 0.7 to 1256%. Since the stiffness of the composite is more at a temperature of 60°C the dynamic intersection between G' and G'' is taking place at a very high strain of around 400%, whereas the same happened at a strain of 69% at 80°C for the first strain sweep. At high temperature (100°C), the viscosity of the composite is extremely low, which allows an easy and maximum orientation of the short fiber in the first strain sweep itself. As a result a marginal growth in the shear storage modulus was noticed in the subsequent strain sweeps as evident from the inset of Figure 12(b). The variation of complex viscosity as a function of an LVE frequency sweep measured before and after the application of an amplitude sweep in the range of 0.7–1256% at 60 and 100°C are displayed in

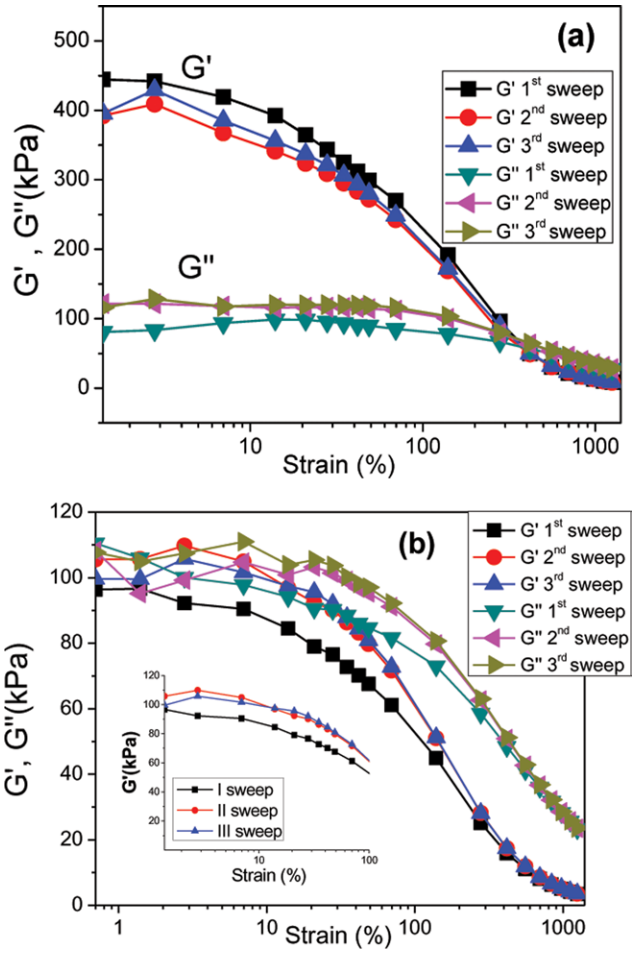

Figure 12. Variation of G' and G'' with repeated strain sweep from 0.7% to 1256%, 0.3Hz (a) at 60°C and (b) at 100°C. Inset shows the variation of G' with strain sweep at 100°C. [Color figure can be viewed in the online issue, which is available at wileyonlinelibrary.com.]

Figure 13(a,b), respectively. It is clear from Figure 13(a) that the complex viscosity measured during the first frequency sweep having no strain history always shows higher value than the subsequent sweeps. This may be due to the severe fiber network break-down and the inability of the short fiber to form a strong continuous fiber string within the composite owing to the high matrix viscosity at 60°C. On the other hand the behavior of complex viscosity with repeated frequency sweep observed at 100°C was exactly similar to those observed at 80°C. However, the magnitudes of the complex viscosity recorded at 100°C are lower than those measured at 80°C because of the lower melt viscosity of the composite at this temperature.

MORPHOLOGICAL ANALYSES

Figure 14(a) represents the optical microscopic (OM) images of the short fiber composite before strain sweep. It is clear from the figure that fibers in the sample before an oscillatory shearing are oriented randomly. This is quite expected and is due to the random orientations formed during the sample preparation by the process of compression molding. The random fiber orientation in the composite we have already confirmed by analyzing the tensile fractured surface of the composite using scanning electron microscopy.[7] Figure 14(b) represents an OM image of a 5 phr short fiber-filled composite taken after the first strain sweep ranges from 0.7 to 1256%. It is clear from the figure that though the fibers are oriented in the direction of the applied oscillatory shear strain; the stacking of the oriented fibers are still not effective. However, a well oriented and a tightly packed oriented fiber structure was found in the OM images of the composite taken after the 4th strain sweep cycle as shown in Figure 14(c). These optical microscopic analyses are very well supported with our previous detailed discussions on the orientational changes of the short fiber from the initial random fiber distribution to the well packed continuous fiber structure with repeated strain sweep in the range 0.7–1256% as demonstrated in Figure 7.

CONCLUSIONS

In this study, the changes in the rheological behavior were primarily explored due to the strain induced fiber orientation at

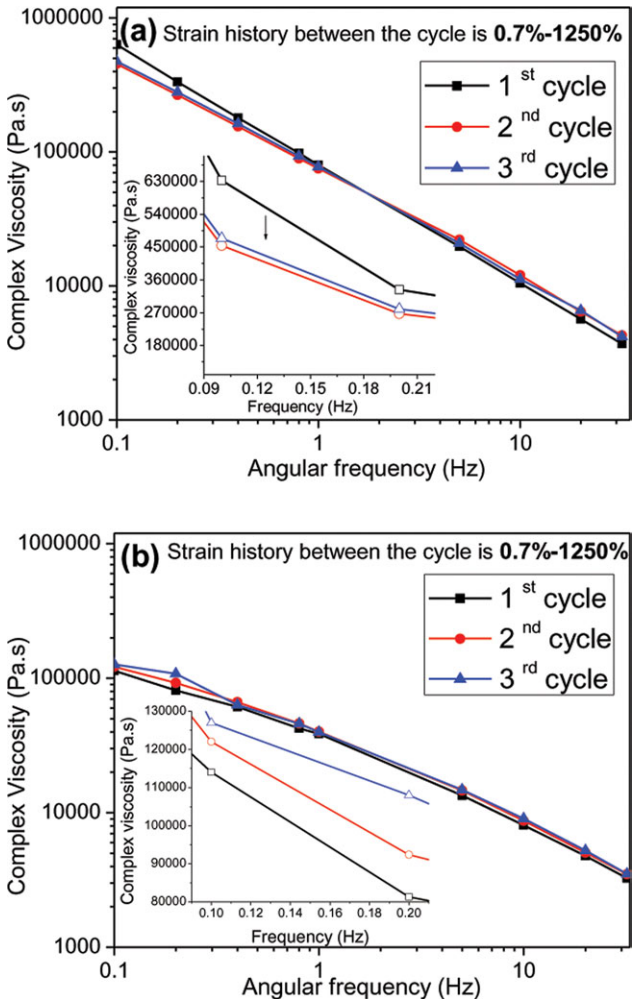

Figure 13. Variation of complex viscosity with repeated frequency sweep having a prestrain history in the range of 0.7–1256% (a) at 60°C and (b) at 100°C. [Color figure can be viewed in the online issue, which is available at wileyonlinelibrary.com.]

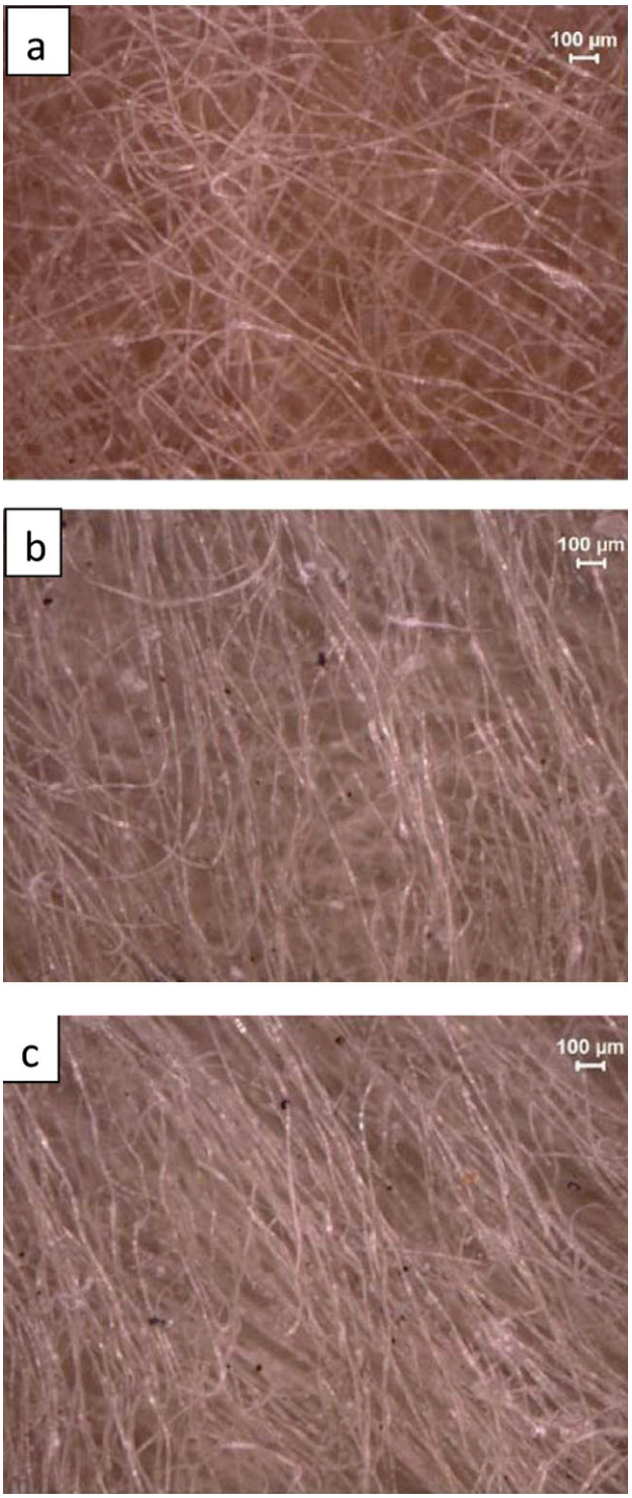

Figure 14. Optical microscopic images of a 5 phr short fiber composite (a) before the strain sweep (b) after the 1st strain sweep and (c) after the 4th strain sweep cycle. [Color figure can be viewed in the online issue, which is available at wileyonlinelibrary.com.]

the high strain regime. Rheological parameters, such as, storage modulus (G'), and complex viscosity (η^*) were mainly determined with repeated strain sweeps of various extent of strains and LVE frequency sweeps as per a specially designed testing protocol using a Rubber Process Analyzer. Our most important finding is that the application of an oscillatory shear strain, especially in the range of 500–1250%, imposing a strong fiber orientation in the circumferential direction leads to a continuous fiber string formation from its randomly distributed state. These fiber strings get thickened for further strain sweeps under the above strain range applied on the sample. As a result, the overall stiffness of the composite in the direction of the shear strain is getting increased. This is evident from the tremendous increase in the elastic shear modulus at the low strain region recorded for the strain sweep from 0.7 to 100% after the application of a strain sweep in the range of 500–1250% applied on the same sample under investigation. The increased complex viscosity of the composite having a prestrain history in the above mentioned strain range (500–1250%) as a function of LVE frequency sweep strongly supports the continuous fiber string formation from the short fiber and its thickening with repeated strain sweep. This observation is of great interest in short fiber filled polymer processing, especially in the hose industry where the circumferential fiber orientation in the direction of extrusion is of prime importance for the hoop reinforcement. Hence this observation may lead to a new way for tool (die) design to increase the fiber orientation in the hoop direction in a short fiber filled elastomer composite for the development of *in-situ* cord reinforced extruded profiles.

ACKNOWLEDGMENTS

The authors are thankful to Teijin Aramid BV, The Netherlands for providing the Technora short fibers.

REFERENCES

1. McNally, T.; Mc Shane, P.; Murphy, W. R.; Millev A. *Polymer* **2002**, *43*, 3785.
2. Babu, R. R.; Singha, N. K.; Naskar, K. *eXpress Polym. Lett.* **2008**, *2*, 226.
3. Nalini, U. R.; Pandurangan, A.; Abdul, S. S. M. *J. Polym. Res.* **2007**, *14*, 441.
4. Echevarria, G. G.; Eguiazabal J. I.; Nazabal, J. *Eur. Polym. J.* **2007**, *43*, 1027.
5. Yu, Z. Z.; Ou, Y. C.; Hu, G. H. *J. Appl. Polym. Sci.* **1998**, *69*, 1711.
6. Chantaratcharoen, A.; Sirisinha, C.; Amornsakchai, T.; Limcharoen, S. B.; Meesiri, W. *J. Appl. Polym. Sci.* **1999**, *74*, 2414.
7. Shibulal, G. S.; Naskar, K. *J. Polym. Res.* **2011**, *18*, 2295.
8. Shibulal, G. S.; Naskar, K. *eXp PolymLett.* **2012**, *6*, 329.
9. Shenoy, A. V. Rheology of Filled Polymer Systems; Kluwer Academic Publishers: London, **1999**; p 40.
10. Leblanc, J. L. *Prog. Polym. Sci.* **2002**, *27*, 627.
11. Nair, K. C. M.; Kumar, R. P.; Thomas, S.; Schit, S. C.; Ramamurthy, K. *Compos. Part A* **2000**, *31*, 1231.
12. Kumar, R. P.; Nair, K. C. M.; Thomas, S.; Schit, S. C.; Ramamurthy, K. *Compos. Sci. Techol.* **2000**, *60*, 1737.

13. Czarnecki, L.; White, J. L. *J. Appl. Polym. Sci.* **1980**, *25*, 1217.
14. Roy, D.; Gupta, B. R. *J. Appl. Polym. Sci.* **1993**, *49*, 1475.
15. Folkes, M. J.; Russell, D. A. M. *Polymer* **1980**, *21*, 1252.
16. Hobbie, E. K. *Rheologica Acta* **2010**, *49*, 323.
17. Kim, J. K.; Song, J. H. *J. Rheol.* **1997**, *41*, 1061.
18. Kim, J. K., Park, S. H. *J. Mater. Sci.* **2000**, *35*, 1069.
19. Bay, R. S.; Tucker, C. *Polym. Eng. Sci.* **1992**, *32*, 240.
20. Ranganathan, S.; Advani, G. S. *J. Polym. Sci. Part. B: Polym. Phy.* **1990**, *28*, 2651.
21. Wang, J.; Geng, C.; Luo, F.; Liu, Y.; Wang, K.; Fu, Q.; He, B. *Mater. Sci. Eng. A* **2011**, *528*, 3169.
22. Zhao, L.; Yang, H.; Song, Y.; Zhou, Y.; Hu, G.; Zheng, Q. *J. Mater. Sci.* **2011**, *46*, 2495.
23. Sternstein, S. S.; Zhu, A. *J. Macromolecules* **2002**, *35*, 7262.
24. Guo, R.; Azaiez, J.; Bellehumeur, C. *Polym. Eng. Sci.* **2005**, *45*, 385.
25. Rajabian, M.; Dubois, C.; Grmela, M.; Carreau, J. P. *Rheologica Acta* **2008**, *47*, 701.
26. Bailly, M.; Kontopoulou, M.; Mabrouk, E. K. *Polymer* **2010**, *51*, 5506.
27. Jamshidi, M.; Taromi, A. F.; Mohammadi, N. *Iranian Polym. J.* **2005**, *14*, 229.
28. Cassagnau, P. *Polymer* **2003**, *44*, 2455.
29. Chazeau, L.; Brown, J. D.; Yanyo, L. C.; Sternstein, S. S. *Polym. Compos.* **2000**, *21*, 202.
30. Malchev, P. G.; Norder, B.; Picken, S. J.; Gotsis, A. D. *J. Rheol.* **2007**, *52*, 235.
31. Flandin, L.; Chang, A.; Nazarenko, S.; Hiltner, A.; Baer, E. *J. Appl. Polym. Sci.* **2000**, *76*, 894.
32. Zhu, Z.; Thompson, T.; Wang, S. Q.; vonMeerwall, E. D.; Halasa, A. *Macromolecules* **2005**, *38*, 8816.
33. Dong, H.; Jacob, K. *Macromolecules* **2003**, *36*, 8881.